Proceedings of the 17th World Congress
The International Federation of Automatic Control
Seoul, Korea, July 6-11, 2008

Predictive PD Control for Teleoperation with Communication Time Delay

Kouei Yoshida * **Toru Namerikawa** *

* *Division of Electrical Engineering and Computer Science, Kanazawa University, Kakuma-machi Kanazawa, 920-1192, JAPAN. email:yoshida@scl.ec.t.kanazawa-u.ac.jp and toru@t.kanazawa-u.ac.jp*

Abstract: This paper deals with a problem of predictive control for nonlinear multi-DOF teleoperation with time varying delay, parametric uncertainties of the robot model and uncertainties of remote environment. The proposed method is combination of the PD control based on the predictors and the adaptive impedance control. Since the predictors are used to simultaneously estimate the master and slave dynamics, the use of the delayed information is avoided. Thus, the performance degradation due to communication time delay can be alleviated. The adaptive impedance control is used to linearize the robot with parametric uncertainties. Proposed predictive PD control method does not require the environmental dynamic model and can achieve the position coordination and the static force reflection in certain conditions. The stability and position coordination are guaranteed by using the Lyapunov theorem. Experimental results show the effectiveness of proposed teleoperation.

Keywords: Teleoperation, Predictive Control, PD Controllers, Adaptive Control, Time Delay

1. INTRODUCTION

Teleoperation system can extend a human's reach to a remote site and has been developed and motivated by large variety of applications (Hokayem et al. [2006]). It is well known that communication delay may destabilize the system and degrade the closed loop performance. Hence it is necessary to improve the closed loop performance while preserving stability.

Stabilization for a teleoperation with time delay has been achieved by the scattering transformation (Chopra et al. [2003], Namerikawa et al. [2006]) and PD control method (Kawada et al. [2008]). However, system performance degradation occurs when the delay is large, because these methods use delayed transmitted information directly and the gain should be low to ensure stability. On the other hand, a predictive control has been proposed to improve the performance of teleoperation while preserving closed loop stability (Sirouspour et al. [2006], Pan et al. [2006]). In (Pan et al. [2006]), the predictive approach is proposed for the impedance control of bilateral drive-by-wire teleoperation systems with time varying delay. However, in this approach, the environmental model is required for the control law, and a nonlinear multi-DOF teleoperation with model parameter uncertainties is not treated. Furthermore, the position coordination problem is not addressed.

In this paper, we address a problem of predictive control for nonlinear multi-DOF teleoperation with time varying delay, parametric uncertainties of the robot model, uncertainties of remote environment. The proposed method is combination of the PD control based on predictors (Pan et al. [2006]) and the adaptive impedance control (Lu et al. [1991]). The predictors are used to simultaneously estimate the master and slave dynamics, and thereby to avoid the use of the delayed information. Thus, the performance degradation due to communication time delay can be alleviated. The adaptive impedance control is used to linearize the robot with parametric uncertainties. Proposed predictive PD control do not require the environmental dynamic model and can achieve position coordination and static force reflection in certain conditions. The stability and position coordination are guaranteed using the Lyapunov stability method. Several experimental results show the effectiveness of our proposed method.

2. PROBLEM FORMULATION

2.1 Dynamics of Teleoperation System

Assuming absence of friction and other disturbances and compensation of gravity effect, the master and slave robot dynamics with n-DOF are described as

$$\begin{cases} \boldsymbol{M_m}(\boldsymbol{q_m})\ddot{\boldsymbol{q}}_{\boldsymbol{m}} + \boldsymbol{C_m}(\boldsymbol{q_m}, \dot{\boldsymbol{q}}_{\boldsymbol{m}})\dot{\boldsymbol{q}}_{\boldsymbol{m}} = \boldsymbol{\tau_m} + \boldsymbol{\tau_{op}} \\ \boldsymbol{M_s}(\boldsymbol{q_s})\ddot{\boldsymbol{q}}_{\boldsymbol{s}} + \boldsymbol{C_s}(\boldsymbol{q_s}, \dot{\boldsymbol{q}}_{\boldsymbol{s}})\dot{\boldsymbol{q}}_{\boldsymbol{s}} = \boldsymbol{\tau_s} - \boldsymbol{\tau_{env}} \end{cases} \tag{1}$$

where the "m" and, "s" denote the master and the slave indexes respectively, $\boldsymbol{q_m},\ \boldsymbol{q_s} \in R^{n\times 1}$ are the joint angle vectors, $\boldsymbol{\tau_m},\ \boldsymbol{\tau_s} \in R^{n\times 1}$ are the input torque vectors, $\boldsymbol{\tau_{op}} \in R^{n\times 1}$ is operational torque vectors applied to the master arm by human operator, $\boldsymbol{\tau_{env}} \in R^{n\times 1}$ is the environmental torque vectors applied to environment by the slave arm, $\boldsymbol{M_m}(\boldsymbol{q_m}),\ \boldsymbol{M_s}(\boldsymbol{q_s}) \in R^{n\times n}$ are the symmetric and positive definite inertia matrices, $\boldsymbol{C_m}(\boldsymbol{q_m}, \dot{\boldsymbol{q}}_{\boldsymbol{m}})\dot{\boldsymbol{q}}_{\boldsymbol{m}},\ \boldsymbol{C_s}(\boldsymbol{q_s}, \dot{\boldsymbol{q}}_{\boldsymbol{s}})\dot{\boldsymbol{q}}_{\boldsymbol{s}} \in R^{n\times 1}$ are the centrifugal and Coriolis torque vectors. Since matrices $\boldsymbol{M_m}, \boldsymbol{M_s}, \boldsymbol{C_m}, \boldsymbol{C_s}$ are linear in terms of the parameters (Sirouspour et al. [2006]), we can write

$$\begin{cases} \boldsymbol{M_m}(\boldsymbol{q_m})\ddot{\boldsymbol{q}}_{\boldsymbol{m}} + \boldsymbol{C_m}(\boldsymbol{q_m}, \dot{\boldsymbol{q}}_{\boldsymbol{m1}})\dot{\boldsymbol{q}}_{\boldsymbol{m2}} = \boldsymbol{Y_m}(\ddot{\boldsymbol{q}}_{\boldsymbol{m}}, \dot{\boldsymbol{q}}_{\boldsymbol{m1}}, \dot{\boldsymbol{q}}_{\boldsymbol{m2}}, \boldsymbol{q_m})\boldsymbol{\theta_m} \\ \boldsymbol{M_s}(\boldsymbol{q_s})\ddot{\boldsymbol{q}}_{\boldsymbol{s}} + \boldsymbol{C_s}(\boldsymbol{q_s}, \dot{\boldsymbol{q}}_{\boldsymbol{s1}})\dot{\boldsymbol{q}}_{\boldsymbol{s2}} = \boldsymbol{Y_s}(\ddot{\boldsymbol{q}}_{\boldsymbol{s}}, \dot{\boldsymbol{q}}_{\boldsymbol{s1}}, \dot{\boldsymbol{q}}_{\boldsymbol{s2}}, \boldsymbol{q_s})\boldsymbol{\theta_s} \end{cases} \tag{2}$$

where $\boldsymbol{Y_m}, \boldsymbol{Y_s} \in R^{n\times m}$ are regressor matrices, $\boldsymbol{\theta_m}, \boldsymbol{\theta_s} \in R^{m\times 1}$ are parameter vectors. In this paper, we treat time varying communication delay with following properties.

Assumption 1. The communication delay between master and slave robot are time varying delay as $T(t)$ which is bounded as

$$0 \le T(t) \le T^* < \infty, \quad |\dot{T}(t)| \le T^+ < 1 \tag{3}$$

where, $T^* \in R > 0$ and $T^+ \in R > 0$ are positive constant

Assumption 2. The communication time delay $T(t)$ can be measured.

In addition, we assume that the operational torque and environmental torque satisfy the following assumption.

Assumption 3. $|\boldsymbol{\tau_i}(t-T(t)) - \boldsymbol{\tau_i}(t)|(i = m, s)$ are bounded at all time. Furthermore, there exist positive constants ρ_τ such that

$$\left\| \begin{bmatrix} \boldsymbol{\tau_{op}} \\ \boldsymbol{\tau_{env}} \end{bmatrix} \right\| \le \rho_\tau \tag{4}$$

2.2 Control Objective

The controller will be designed to achieve the following objective.

Control Objective:
1) (Stability) The velocities and position coordination error are bounded under the time varying communication delay
2) (Master-Slave Position Coordination) If $\boldsymbol{\tau_{op}} = \boldsymbol{\tau_{env}} = 0$, the position coordination error converge to zero as follows.

$$\boldsymbol{q_m}(t) - \boldsymbol{q_s}(t) \rightarrow \ 0 \ as \ t \rightarrow \infty \tag{5}$$

3) (Static Force Reflection) When $\dot{\boldsymbol{q}}_s = \dot{\boldsymbol{q}}_m = \ddot{\boldsymbol{q}}_s = \ddot{\boldsymbol{q}}_m = 0$, the contact force in slave side are accurately transmitted to the human operator in the master side as $\boldsymbol{\tau_{op}} = \boldsymbol{\tau_{env}}$.
4) (Realization of the Delay-free Dynamics)The Delay-free dynamics is realized even in the presense of delay.

The control objectives 1), 2) and 3) are same with Kawada et al. [2008]. These objectives mean the achievement of transparency. The control objective 4) means decrease of the performance degradation.

3. CONTROLLER DESIGNS

3.1 Control Structure

We propose a novel predictive control method which is combination of the adaptive impedance control and PD control based on predictors. The control structure is shown in Fig. 1. The proposed controllers consist of three parts , "Predictor" , "Trajectory generator" and "Adaptive controller". These blocks of "Trajectory generator" and "Adaptive controller" perform impedance shaping and PD control by using the adaptive impedance control framework. These blocks of "Predictor" predict the master and slave current state in the slave and master side to avoid the use of the delayed information.

3.2 Impedance Shaping by Adaptive Impedance Control

In this subsection, we address a linearization by the adaptive impedance control. In the adaptive impedance control (Lu et al. [1991]) framework, the reference trajectory is generated based on the target impedance and the passivity-based adaptive controller drives the robot to follow the generated reference trajectory in order to realize the target impedance.

According to the adaptive impedance control framework, following input torque is given to master and slave.

$$\boldsymbol{\tau_m} = -\boldsymbol{\tau_{op}} + \boldsymbol{Y_m}(\ddot{\boldsymbol{q}}_{mr}, \dot{\boldsymbol{q}}_m, \dot{\boldsymbol{q}}_{mr}, \boldsymbol{q_m})\overline{\boldsymbol{\theta}}_m - \boldsymbol{K_m}\boldsymbol{r}_m \tag{6}$$
$$\dot{\overline{\boldsymbol{\theta}}}_m = -\boldsymbol{\Gamma_m}\boldsymbol{Y}_m^T(\ddot{\boldsymbol{q}}_{mr}, \dot{\boldsymbol{q}}_m, \dot{\boldsymbol{q}}_{mr}, \boldsymbol{q_m})\boldsymbol{r_m} \tag{7}$$
$$\boldsymbol{\tau_s} = \boldsymbol{\tau_{env}} + \boldsymbol{Y_s}(\ddot{\boldsymbol{q}}_{sr}, \dot{\boldsymbol{q}}_s, \dot{\boldsymbol{q}}_{sr}, \boldsymbol{q_s})\overline{\boldsymbol{\theta}}_s - \boldsymbol{K_s}\boldsymbol{r_s} \tag{8}$$
$$\dot{\overline{\boldsymbol{\theta}}}_s = -\boldsymbol{\Gamma_s}\boldsymbol{Y}_s^T(\ddot{\boldsymbol{q}}_{sr}, \dot{\boldsymbol{q}}_s, \dot{\boldsymbol{q}}_{sr}, \boldsymbol{q_s})\boldsymbol{r_s} \tag{9}$$

where,

$$\begin{cases} \boldsymbol{e_m} = \boldsymbol{q_m} - \boldsymbol{q_{md}} \\ \boldsymbol{e_s} = \boldsymbol{q_s} - \boldsymbol{q_{sd}} \end{cases}, \quad \begin{cases} \dot{\boldsymbol{q}}_{mr} = \dot{\boldsymbol{q}}_{md} - \boldsymbol{\Lambda_m}\boldsymbol{e_m} \\ \dot{\boldsymbol{q}}_{sr} = \dot{\boldsymbol{q}}_{sd} - \boldsymbol{\Lambda_s}\boldsymbol{e_s} \end{cases} \tag{10}$$
$$\begin{cases} \boldsymbol{r_m} = \dot{\boldsymbol{e}}_m + \boldsymbol{\Lambda_m}\boldsymbol{e_m} \\ \boldsymbol{r_s} = \dot{\boldsymbol{e}}_s + \boldsymbol{\Lambda_s}\boldsymbol{e_s}, \end{cases} \tag{11}$$

$\boldsymbol{K_m}, \boldsymbol{K_s}, \boldsymbol{\Lambda_m}, \boldsymbol{\Lambda_s} \in R^{n\times n}$ are diagonal matrices, $\overline{\boldsymbol{\theta}}_m, \overline{\boldsymbol{\theta}}_s \in R^{m\times 1}$ are the estimated parameter vectors, $\boldsymbol{\Gamma_m}, \boldsymbol{\Gamma_s} \in R^{m\times m}$ are positive definite matrix. $\boldsymbol{q_{md}}, \dot{\boldsymbol{q}}_{md}, \ddot{\boldsymbol{q}}_{md}$, $\boldsymbol{q_{sd}}, \dot{\boldsymbol{q}}_{sd}, \ddot{\boldsymbol{q}}_{sd}$ are the trajectories computed according to following linear equations

$$\overline{\boldsymbol{M}}_m\ddot{\boldsymbol{q}}_{md} + \overline{\boldsymbol{B}}_m\dot{\boldsymbol{q}}_{md} = \boldsymbol{\tau_{md}} + \boldsymbol{\tau_{op}} \tag{12}$$
$$\overline{\boldsymbol{M}}_s\ddot{\boldsymbol{q}}_{sd} + \overline{\boldsymbol{B}}_s\dot{\boldsymbol{q}}_{sd} = \boldsymbol{\tau_{sd}} - \boldsymbol{\tau_{env}} \tag{13}$$
$$\boldsymbol{q_{id}}(0) = \boldsymbol{q_i}(0), \quad \dot{\boldsymbol{q}}_{id}(0) = \dot{\boldsymbol{q}}_i(0) \quad (i = m, s)$$

where $\overline{\boldsymbol{M}_m}$, $\overline{\boldsymbol{M}_s}$ are desired inertia and $\overline{\boldsymbol{B}}_m, \overline{\boldsymbol{B}}_s$ are desired damping, $\boldsymbol{\tau_{md}}, \boldsymbol{\tau_{sd}}$ are new control input given in next subsection.

Combining the control law (6)(8) with dynamics (1) yields

$$\begin{cases} \boldsymbol{M_m}(\boldsymbol{q_m})\dot{\boldsymbol{r}}_m + \boldsymbol{C_m}(\boldsymbol{q_m}, \dot{\boldsymbol{q}}_m)\boldsymbol{r_m} + \boldsymbol{K_m}\boldsymbol{r_m} \\ = \boldsymbol{Y_m}(\ddot{\boldsymbol{q}}_{mr}, \dot{\boldsymbol{q}}_m, \dot{\boldsymbol{q}}_{mr}, \boldsymbol{q_m})\tilde{\boldsymbol{\theta}}_m \\ \boldsymbol{M_s}(\boldsymbol{q_s})\dot{\boldsymbol{r}}_s + \boldsymbol{C_s}(\boldsymbol{q_s}, \dot{\boldsymbol{q}}_s)\boldsymbol{r_s} + \boldsymbol{K_s}\boldsymbol{r_s} \\ = \boldsymbol{Y_s}(\ddot{\boldsymbol{q}}_{sr}, \dot{\boldsymbol{q}}_s, \dot{\boldsymbol{q}}_{sr}, \boldsymbol{q_s})\tilde{\boldsymbol{\theta}}_s \end{cases} \tag{14}$$

where $\tilde{\boldsymbol{\theta}} = \overline{\boldsymbol{\theta}} - \boldsymbol{\theta}$ are the parameter estimation error vector. Using this control law, the signals $\boldsymbol{e_m}, \dot{\boldsymbol{e}}_m, \boldsymbol{e_s}, \dot{\boldsymbol{e}}_s$ converge to zero as following lemma.

Lemma 1. (Lu et al. [1991]) Consider the system described by (14) and the parameter adaptation law (7)(9). Assuming $\boldsymbol{q_{id}}, \dot{\boldsymbol{q}}_{id}, \ddot{\boldsymbol{q}}_{id} (i = m, s)$ are bounded, then, the origin of $\boldsymbol{e_m}, \dot{\boldsymbol{e}}_m, \boldsymbol{e_s}, \dot{\boldsymbol{e}}_s$ are asymptotically stable, i.e.,

$$\lim_{t\rightarrow\infty} \boldsymbol{e_m}, \dot{\boldsymbol{e}}_m, \boldsymbol{e_s}, \dot{\boldsymbol{e}}_s = 0. \tag{15}$$

proof : This lemma can be proven easily by the Lyapunov function candidate $V_i = \frac{1}{2}\boldsymbol{r}_i^T\boldsymbol{M_i}\boldsymbol{r_i} + \frac{1}{2}\tilde{\boldsymbol{\theta}}_i^T\boldsymbol{\Gamma}_i^{-1}\tilde{\boldsymbol{\theta}}_i \ \ (i = m, s)$. □

From this lemma, the master and slave track to trajectories $\boldsymbol{q_{md}}, \boldsymbol{q_{sd}}$ even in the presence of the parametric uncertainties. Thus, the control problem of nonlinear dynamics (1) has been transformed into a control problem of linear systems (12)(13).

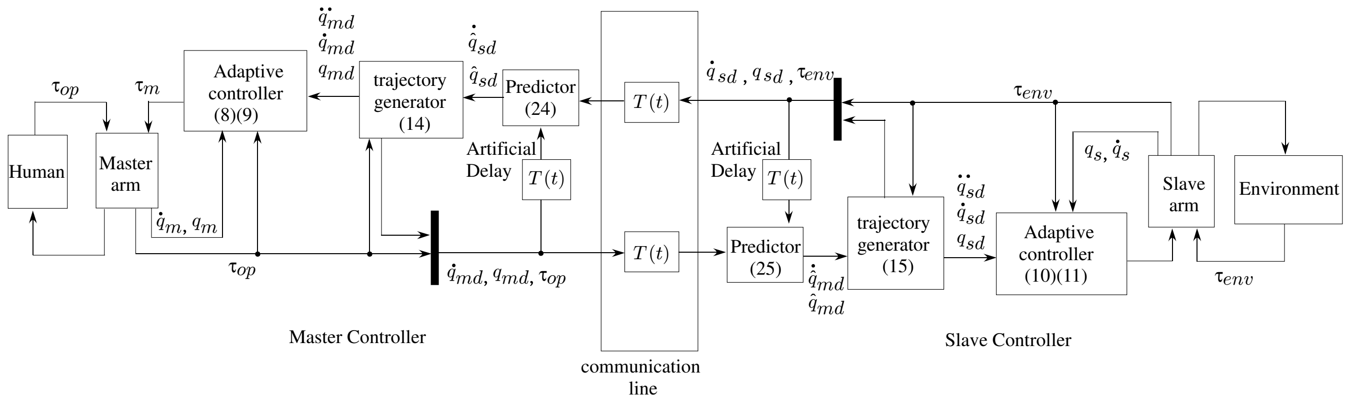

Fig. 1. Control structure

3.3 PD Control with Predicted Value

To avoid the performance degradation caused by the delay, the new control input is given as following PD control law

$$\boldsymbol{\tau_{md}} = \boldsymbol{K_p}\{\boldsymbol{\hat{q}_{sd}} - \boldsymbol{q_{md}}\} + \boldsymbol{K_d}\{\boldsymbol{\dot{\hat{q}}_{sd}} - \boldsymbol{\dot{q}_{md}}\} \tag{16}$$

$$\boldsymbol{\tau_{sd}} = \boldsymbol{K_p}\{\boldsymbol{\hat{q}_{md}} - \boldsymbol{q_{sd}}\} + \boldsymbol{K_d}\{\boldsymbol{\dot{\hat{q}}_{md}} - \boldsymbol{\dot{q}_{sd}}\} \tag{17}$$

where $\boldsymbol{K_p}, \boldsymbol{K_d} \in R^{n\times n} > 0$ are the proportional and derivative gains respectively, $\boldsymbol{\hat{q}_{md}}, \boldsymbol{\hat{q}_{sd}}, \boldsymbol{\dot{\hat{q}}_{md}}, \boldsymbol{\dot{\hat{q}}_{sd}}$ are the predicted value of $\boldsymbol{q_{md}}, \boldsymbol{q_{sd}}, \boldsymbol{\dot{q}_{md}}, \boldsymbol{\dot{q}_{sd}}$ obtained by the predictors mentioned in next subsection. Combining the new control input (16)(17) with the linearized dynamics (12)(13) yields

$$\begin{aligned}\boldsymbol{\overline{M}_m}\boldsymbol{\ddot{q}_{md}} + \boldsymbol{\overline{B}_m}\boldsymbol{\dot{q}_{md}} = {} & \boldsymbol{K_p}\{\boldsymbol{q_{sd}} - \boldsymbol{q_{md}}\} + \boldsymbol{K_d}\{\boldsymbol{\dot{q}_{sd}} - \boldsymbol{\dot{q}_{md}}\} + \boldsymbol{\tau_{op}} \\ & \underbrace{+\boldsymbol{K_p}\{\boldsymbol{\hat{q}_{sd}} - \boldsymbol{q_{sd}}\} + \boldsymbol{K_d}\{\boldsymbol{\dot{\hat{q}}_{sd}} - \boldsymbol{\dot{q}_{sd}}\}}_{\text{Effect of prediction error}}\end{aligned} \tag{18}$$

$$\begin{aligned}\boldsymbol{\overline{M}_s}\boldsymbol{\ddot{q}_{sd}} + \boldsymbol{\overline{B}_s}\boldsymbol{\dot{q}_{sd}} = {} & \boldsymbol{K_p}\{\boldsymbol{q_{md}} - \boldsymbol{q_{sd}}\} + \boldsymbol{K_d}\{\boldsymbol{\dot{q}_{md}} - \boldsymbol{\dot{q}_{sd}}\} - \boldsymbol{\tau_{env}} \\ & \underbrace{+\boldsymbol{K_p}\{\boldsymbol{\hat{q}_{md}} - \boldsymbol{q_{md}}\} + \boldsymbol{K_d}\{\boldsymbol{\dot{\hat{q}}_{md}} - \boldsymbol{\dot{q}_{md}}\}}_{\text{Effect of prediction error}}.\end{aligned} \tag{19}$$

Above system can be interpreted as "Delay-free PD controlled system dynamics + Effect of prediction error". Thus, if the prediction error is small, the performance degradation due to the delay is alleviated and the control objective 4) is achieved.

3.4 Predictor Design

A goal of the predictor design is to generate the $\boldsymbol{\dot{\hat{q}}_{sd}}$,$\boldsymbol{\hat{q}_{sd}}$ at the master side and $\boldsymbol{\dot{\hat{q}}_{md}}, \boldsymbol{\hat{q}_{md}}$ at the slave side. Defining the state vectors as

$$\boldsymbol{z_{md}} = \begin{bmatrix}\boldsymbol{q_{md}} \\ \boldsymbol{\dot{q}_{md}}\end{bmatrix}, \boldsymbol{z_{sd}} = \begin{bmatrix}\boldsymbol{q_{sd}} \\ \boldsymbol{\dot{q}_{sd}}\end{bmatrix},$$

the state space representation of (18)(19) are given as

$$\boldsymbol{\dot{z}_{md}} = \boldsymbol{A_m}\boldsymbol{z_{md}} + \boldsymbol{B_{m1}}\boldsymbol{\tau_{op}} + \boldsymbol{B_{m2}}\boldsymbol{\hat{z}_{sd}} \tag{20}$$

$$\boldsymbol{\dot{z}_{sd}} = \boldsymbol{A_s}\boldsymbol{z_{sd}} + \boldsymbol{B_{s1}}\boldsymbol{\tau_{env}} + \boldsymbol{B_{s2}}\boldsymbol{\hat{z}_{md}} \tag{21}$$

where

$$\boldsymbol{\hat{z}_{md}} = \begin{bmatrix}\boldsymbol{\hat{q}_{md}} \\ \boldsymbol{\dot{\hat{q}}_{md}}\end{bmatrix}, \boldsymbol{\hat{z}_{sd}} = \begin{bmatrix}\boldsymbol{\hat{q}_{sd}} \\ \boldsymbol{\dot{\hat{q}}_{sd}}\end{bmatrix}$$

$$\boldsymbol{A_m} = \begin{bmatrix}\boldsymbol{0} & \boldsymbol{I} \\ -\boldsymbol{\overline{M}_m^{-1}}\boldsymbol{K_p} & -\boldsymbol{\overline{M}_m^{-1}}(\boldsymbol{\overline{B}_m} + \boldsymbol{K_d})\end{bmatrix}$$

$$\boldsymbol{B_{m1}} = \begin{bmatrix}\boldsymbol{0} \\ \boldsymbol{\overline{M}_m^{-1}}\end{bmatrix}, \boldsymbol{B_{m2}} = \begin{bmatrix}\boldsymbol{0} & \boldsymbol{0} \\ \boldsymbol{\overline{M}_m^{-1}}\boldsymbol{K_p} & \boldsymbol{\overline{M}_m^{-1}}\boldsymbol{K_d}\end{bmatrix}$$

$$\boldsymbol{A_s} = \begin{bmatrix}\boldsymbol{0} & \boldsymbol{I} \\ -\boldsymbol{\overline{M}_s^{-1}}\boldsymbol{K_p} & -\boldsymbol{\overline{M}_s^{-1}}(\boldsymbol{\overline{B}_s} + \boldsymbol{K_d})\end{bmatrix}$$

$$\boldsymbol{B_{s1}} = \begin{bmatrix}\boldsymbol{0} \\ -\boldsymbol{\overline{M}_s^{-1}}\end{bmatrix}, \boldsymbol{B_{s2}} = \begin{bmatrix}\boldsymbol{0} & \boldsymbol{0} \\ \boldsymbol{\overline{M}_s^{-1}}\boldsymbol{K_p} & \boldsymbol{\overline{M}_s^{-1}}\boldsymbol{K_d}\end{bmatrix}$$

where $\boldsymbol{I}$ is identity matrix. Using above equation (20)(21), The predictors are given the following structure (Pan et al. [2006])

- The master side predictors

$$\begin{cases}\boldsymbol{\dot{\hat{z}}_{md}} = & \boldsymbol{A_m}\boldsymbol{\hat{z}_{md}} + \boldsymbol{B_{m1}}\boldsymbol{\tau_{op}}(t - \overline{T}(t)) + \boldsymbol{B_{m2}}\boldsymbol{\hat{z}_{sd}} \\ & +\boldsymbol{E_m}\{\boldsymbol{\hat{z}_{md}}(t - \overline{T}(t)) - \boldsymbol{z_{md}}(t - \overline{T}(t))\} \\ \boldsymbol{\dot{\hat{z}}_{sd}} = & \boldsymbol{A_s}\boldsymbol{\hat{z}_{sd}} + \boldsymbol{B_{s1}}\boldsymbol{\tau_{env}}(t - T(t)) + \boldsymbol{B_{s2}}\boldsymbol{\hat{z}_{md}} \\ & +\boldsymbol{E_s}\{\boldsymbol{\hat{z}_{sd}}(t - \overline{T}(t)) - \boldsymbol{z_{sd}}(t - T(t))\}\end{cases} \tag{22}$$

- The slave side predictors

$$\begin{cases}\boldsymbol{\dot{\hat{z}}_{md}} = & \boldsymbol{A_m}\boldsymbol{\hat{z}_{md}} + \boldsymbol{B_{m1}}\boldsymbol{\tau_{op}}(t - T(t)) + \boldsymbol{B_{m2}}\boldsymbol{\hat{z}_{sd}} \\ & +\boldsymbol{E_m}\{\boldsymbol{\hat{z}_{md}}(t - \overline{T}(t)) - \boldsymbol{z_{md}}(t - T(t))\} \\ \boldsymbol{\dot{\hat{z}}_{sd}} = & \boldsymbol{A_s}\boldsymbol{\hat{z}_{sd}} + \boldsymbol{B_{s1}}\boldsymbol{\tau_{env}}(t - \overline{T}(t)) + \boldsymbol{B_{s2}}\boldsymbol{\hat{z}_{md}} \\ & +\boldsymbol{E_s}\{\boldsymbol{\hat{z}_{sd}}(t - \overline{T}(t)) - \boldsymbol{z_{sd}}(t - \overline{T}(t))\}\end{cases} \tag{23}$$

where $\boldsymbol{E_m}, \boldsymbol{E_s} \in R^{2n\times 2n}$ are gains to correct prediction errors. In the equations (22)(23), The notation $(t - T(t))$ represents the signal delayed by communication line, and the notation $(t - \overline{T}(t))$ represents the signal delayed artificially by calculator. Under *Assumption 2*, it is easy to select as $\overline{T}(t) = T(t)$. Thus, the equations (22)(23) become same dynamics and the predictied values become same values in both side.

Next, we consider the dynamics of prediction error. Considering that the equations (22) are same as the equations (23) under *Assumption 2* and subtracting (20)(21) from (22), then the following prediction error dynamics is obtained.

$$\boldsymbol{\dot{\tilde{z}}_d} = \boldsymbol{A}\boldsymbol{\tilde{z}_d} + \boldsymbol{E}\boldsymbol{\tilde{z}_d}(t - T) + \boldsymbol{d} \tag{24}$$

where,

$$\boldsymbol{\tilde{z}_d} = \begin{bmatrix}\boldsymbol{\hat{z}_{md}} - \boldsymbol{z_{md}} \\ \boldsymbol{\hat{z}_{sd}} - \boldsymbol{z_{sd}}\end{bmatrix}, \boldsymbol{A} = \begin{bmatrix}\boldsymbol{A_m} & 0 \\ 0 & \boldsymbol{A_s}\end{bmatrix}, \boldsymbol{E} = \begin{bmatrix}\boldsymbol{E_m} & 0 \\ 0 & \boldsymbol{E_s}\end{bmatrix}$$

$$\boldsymbol{d} = \begin{bmatrix}\boldsymbol{B_{m1}}(\boldsymbol{\tau_{op}}(t - T(t)) - \boldsymbol{\tau_{op}}(t)) \\ \boldsymbol{B_{s1}}(\boldsymbol{\tau_{env}}(t - T(t)) - \boldsymbol{\tau_{env}}(t))\end{bmatrix}. \tag{25}$$

$\boldsymbol{d}$ is seen here as a disturbance. Under the *Assumption 3*, the vector $\boldsymbol{d}$ is bounded. Since $\boldsymbol{A}$ is stable matrix and $\boldsymbol{d}$ is bounded, the stability of the predictor can be ensured even if $\boldsymbol{E} = 0$. Nevertheless, it is possible to design a gain $\boldsymbol{E}$ such that the performance of the predictor can be improved (Pan et al. [2006]). The stability of the prediction error dynamics is guaranteed as following lemma.

Lemma 2. (Pan et al. [2006]) Assume that $\boldsymbol{A}+\boldsymbol{E}$ is stable. Given $\gamma_p > 0$, if there exists $\boldsymbol{P_1} = \boldsymbol{P_1}^T > 0, r_1 > 0, r_2 > 0$, such that

$$\boldsymbol{\mathcal{L}_1} = \begin{bmatrix} \boldsymbol{\Xi} & \boldsymbol{P_1 E} & \boldsymbol{P_1 E} & \boldsymbol{P_1 E} & \boldsymbol{P_1} \\ \boldsymbol{E}^T \boldsymbol{P_1} & \boldsymbol{\psi_1} & 0 & 0 & 0 \\ \boldsymbol{E}^T \boldsymbol{P_1} & 0 & \boldsymbol{\psi_1} & 0 & 0 \\ \boldsymbol{E}^T \boldsymbol{P_1} & 0 & 0 & -\gamma^2 T^{*-1} & 0 \\ \boldsymbol{P_1} & 0 & 0 & 0 & -\gamma^2 \boldsymbol{I} \end{bmatrix} < 0 \tag{26}$$

where

$$\boldsymbol{\Xi} = (\boldsymbol{A}+\boldsymbol{E})^T \boldsymbol{P_1} + \boldsymbol{P_1}(\boldsymbol{A}+\boldsymbol{E}) + T^* r_1 \boldsymbol{A}^T \boldsymbol{A} + ((T^*)/(1-T^+) + T^*) r_2 \boldsymbol{E}^T \boldsymbol{E} \tag{27}$$

$$\boldsymbol{\psi_1} = -r_1(1-T^+)T^{*-1}\boldsymbol{I}, \quad \boldsymbol{\psi_2} = -r_2(1-T^+)^2 T^{*-1}\boldsymbol{I}, \tag{28}$$

then, system (24) is stable. Furthermore, if $\| \boldsymbol{d} \|$ is bounded, there exist positive constant ρ_p satisfying

$$\| \tilde{\boldsymbol{z}}_{\boldsymbol{d}} \| \leq \rho_p. \tag{29}$$

From *Lemma 2*, the prediction error converge to zero when $\boldsymbol{d} = 0$. On the other hand, if $\boldsymbol{d} \neq 0$, The prediction error may not converge, but is bounded.

Remark 1. When the delays are asymmetric (i.e., forward delay $\neq$ backward delay) and not measurable, we can discuss similarly by using time-stamping and artificial delay up to maximum delay T^*(Kosuge et al. [1996]).

4. STABILITY ANALYSIS

In this section, we present the stability of the teleoperation system. To facilitate the stability analysis, we introduce the state space representations of (18)(19) as follows

$$\dot{\boldsymbol{X}}_{\boldsymbol{d}} = \boldsymbol{A_e X_d} + \boldsymbol{B_e \tau} + \boldsymbol{D_e} \tilde{\boldsymbol{z}}_{\boldsymbol{d}} \tag{30}$$

where

$$\boldsymbol{\tau} = \begin{bmatrix} \boldsymbol{\tau_{op}} \\ -\boldsymbol{\tau_{env}} \end{bmatrix}, \boldsymbol{B_e} = \begin{bmatrix} \overline{\boldsymbol{M}}_{\boldsymbol{m}}^{-1} & 0 \\ 0 & \overline{\boldsymbol{M}}_{\boldsymbol{s}}^{-1} \\ 0 & 0 \end{bmatrix}, \boldsymbol{X_d} = \begin{bmatrix} \dot{\boldsymbol{q}}_{\boldsymbol{md}} \\ \dot{\boldsymbol{q}}_{\boldsymbol{sd}} \\ \boldsymbol{q_{md}} - \boldsymbol{q_{sd}} \end{bmatrix},$$

$$\boldsymbol{A_e} = \begin{bmatrix} -\overline{\boldsymbol{M}}_{\boldsymbol{m}}^{-1}(\boldsymbol{B_m}+\boldsymbol{K_d}) & \overline{\boldsymbol{M}}_{\boldsymbol{m}}^{-1}\boldsymbol{K_d} & -\overline{\boldsymbol{M}}_{\boldsymbol{m}}^{-1}\boldsymbol{K_p} \\ \overline{\boldsymbol{M}}_{\boldsymbol{s}}^{-1}\boldsymbol{K_d} & -\overline{\boldsymbol{M}}_{\boldsymbol{s}}^{-1}(\boldsymbol{B_s}+\boldsymbol{K_d}) & \overline{\boldsymbol{M}}_{\boldsymbol{m}}^{-1}\boldsymbol{K_p} \\ \boldsymbol{I} & -\boldsymbol{I} & 0 \end{bmatrix},$$

$$\boldsymbol{D_e} = \begin{bmatrix} 0 & 0 & \overline{\boldsymbol{M}}_{\boldsymbol{m}}^{-1}\boldsymbol{K_p} & \overline{\boldsymbol{M}}_{\boldsymbol{m}}^{-1}\boldsymbol{K_d} \\ \overline{\boldsymbol{M}}_{\boldsymbol{s}}^{-1}\boldsymbol{K_p} & \overline{\boldsymbol{M}}_{\boldsymbol{m}}^{-1}\boldsymbol{K_d} & 0 & 0 \\ 0 & 0 & 0 & 0 \end{bmatrix}.$$

Furthermore, We also define the vector $\boldsymbol{X}$ as follows

$$\boldsymbol{X} = \begin{bmatrix} \dot{\boldsymbol{q}}_{\boldsymbol{m}} \\ \dot{\boldsymbol{q}}_{\boldsymbol{s}} \\ \boldsymbol{q_m} - \boldsymbol{q_s} \end{bmatrix}. \tag{31}$$

From this definition, boundedness of $\| \boldsymbol{X} \|$ imply the boundedness of the velocity $\dot{\boldsymbol{q}}_{\boldsymbol{m}}, \dot{\boldsymbol{q}}_{\boldsymbol{s}}$ and the position error $\boldsymbol{q_m} - \boldsymbol{q_s}$. Furthermore, $\| \boldsymbol{X} \| \to 0$ imply $\dot{\boldsymbol{q}}_{\boldsymbol{m}}, \dot{\boldsymbol{q}}_{\boldsymbol{s}}, \boldsymbol{q_m} - \boldsymbol{q_s} \to 0$, i.e. the position coodination. The stability of the system and the position coordination are concluded in the following theorem.

Theorem 1. Considering the teleoperation controlled by proposed controller.

1)(stability) $\| \boldsymbol{X} \|$ is bounded and tends, in steady state, to a ball B_r

$$B_r = \left\{ \tilde{\boldsymbol{X}} : \| \tilde{\boldsymbol{X}} \| \leq \sqrt{\gamma_1^2 \rho_\tau^2 + \gamma_2^2 \rho_p^2} \sqrt{\frac{\lambda_{max}\boldsymbol{P_2}}{\lambda_{min}\boldsymbol{P_2}}} \right\} \tag{32}$$

where, $\rho_\tau, \rho_p > 0$ are constants obtained from the *Assumption 3*, *Lemma 2*. $\boldsymbol{P_2} \in R^{3n \times 3n}$, $\boldsymbol{P_2} = \boldsymbol{P^T} > 0$ is solution of following LMI given $\gamma_1, \gamma_2 > 0$.

$$\begin{bmatrix} \boldsymbol{A_e^T P_2} + \boldsymbol{P_2 A_e} + \boldsymbol{I} & \boldsymbol{P_2 B_e} & \boldsymbol{P_2 D_e} \\ \boldsymbol{B_e}^{\boldsymbol{T}} \boldsymbol{P_2} & -\gamma_1^2 \boldsymbol{I} & 0 \\ \boldsymbol{D_e}^{\boldsymbol{T}} \boldsymbol{P_2} & 0 & -\gamma_2^2 \boldsymbol{I} \end{bmatrix} < 0 \tag{33}$$

$\lambda_{max}\boldsymbol{P_2}$,$\lambda_{min}\boldsymbol{P_2}$ are maximum eigenvalue and minimum eigenvalue of $\boldsymbol{P_2}$ respectively.

2)(position coordination) If $\boldsymbol{\tau_{op}}, \boldsymbol{\tau_{env}} = 0$, then, $\lim_{t\to\infty} \| \boldsymbol{X} \| = 0$. Namely the position coordination is achieved.

proof : 1) The norm $\| \boldsymbol{X} \|$ satisfy the following inequality from the property of norm.

$$\| \boldsymbol{X} \| = \| \boldsymbol{X} - \boldsymbol{X_d} + \boldsymbol{X_d} \| \leq \| \boldsymbol{X} - \boldsymbol{X_d} \| + \| \boldsymbol{X_d} \| \tag{34}$$

The first term of right hand in above inequality, i.e., the term $\| \boldsymbol{X} - \boldsymbol{X_d} \|$, consists of $\boldsymbol{e_m}, \boldsymbol{e_m}, \dot{\boldsymbol{e}}_{\boldsymbol{m}}, \dot{\boldsymbol{e}}_{\boldsymbol{s}}$ as

$$\| \boldsymbol{X} - \boldsymbol{X_d} \| = \sqrt{\| \dot{\boldsymbol{e}}_{\boldsymbol{m}} \|^2 + \| \dot{\boldsymbol{e}}_{\boldsymbol{s}} \|^2 + \| \boldsymbol{e_m} - \boldsymbol{e_s} \|^2}.$$

Using $\lim_{t\to\infty} \boldsymbol{e_m}, \boldsymbol{e_m}, \dot{\boldsymbol{e}}_{\boldsymbol{m}}, \dot{\boldsymbol{e}}_{\boldsymbol{s}} = 0$, from *Lemma 1*, we have

$$\lim_{t\to\infty} \| \boldsymbol{X} - \boldsymbol{X_d} \| = 0. \tag{35}$$

Next, we consider second term of right hand in (34), i.e., the term $\| \boldsymbol{X_d} \|$. Define a Lyapunov function as $V_1 = \boldsymbol{X_d^T P_2 X_d}$. The derivative of this function along the trajectories is given by

$$\dot{V}_1 = \boldsymbol{X_d^T}(\boldsymbol{P_2 A_e} + \boldsymbol{A_e^T P_2})\boldsymbol{X_d} + \boldsymbol{X_d^T P_2 B_e \tau} + \boldsymbol{\tau}^T \boldsymbol{B_e^T P_2 X_d} + \boldsymbol{X_d^T P_2 D_e} \tilde{\boldsymbol{z}}_{\boldsymbol{d}} + \tilde{\boldsymbol{z}}_{\boldsymbol{d}}^T \boldsymbol{D_e^T P_2 X_d} \tag{36}$$

$$\leq \boldsymbol{X_d^T}(\boldsymbol{P A_e} + \boldsymbol{A_e^T P_2} + \gamma_1^{-2} \boldsymbol{P_2 B_e B_e^T P_2} + \gamma_2^{-2} \boldsymbol{P_2 D_e D_e^T P_2} + \boldsymbol{I})\boldsymbol{X_d} - \| \boldsymbol{X_d} \|^2 + \gamma_1^2 \| \boldsymbol{\tau} \|^2 + \gamma_2^2 \| \tilde{\boldsymbol{z}}_{\boldsymbol{d}} \|^2 \tag{37}$$

Since the LMI (33) imply $\boldsymbol{P_2 A_e} + \boldsymbol{A_e^T P_2} + \gamma_1^{-2} \boldsymbol{P_2 B_e B_e^T P_2} + \gamma_2^{-2} \boldsymbol{P_2 D_e D_e^T P_2} + \boldsymbol{I} < 0$, and $\| \boldsymbol{\tau} \|$, $\| \tilde{\boldsymbol{z}}_{\boldsymbol{d}} \|$, satisfy (4)(29), we have following equation

$$\dot{V}_1 \leq -\| \boldsymbol{X_d} \|^2 + \gamma_1^2 \rho_\tau^2 + \gamma_2^2 \rho_p^2$$

From this inequality and Lyapunov theory, $\| \boldsymbol{X_d} \|$ is bounded and tend to a ball B_r. From boundedness of $\| \boldsymbol{X_d} \|$ and equations (34) and (35), we can conclude that $\| \boldsymbol{X} \|$ is also bounded and tends to a ball B_r in steady state. Thus, the position error and the velocities are bounded.

2)When $\boldsymbol{\tau_{op}}, \boldsymbol{\tau_{env}} = 0$, the dynamics of (30) and the prediction error dynamics (24) become

$$\dot{X}_d = A_e X_d + D_e \tilde{z}_d,\ \tilde{z}_d = A\tilde{z}_d + E\tilde{z}_d(t-T) \quad (38)$$

Considering positive definite function as $V_2 = X_d^T P_2 X_d + (\gamma_2^2+1)V_p$ where, V_p is the Lyapunov-Krasovskii function used to prove *Lemma 2*, defined as follows(Pan et al. [2006])

$$\begin{aligned} V_p &= \tilde{z}_d^T P_1 \tilde{z}_d + \int_{t-T(t)}^{t}\int_{\theta}^{t} r_1 \tilde{z}_d^T(s) A^T A \tilde{z}_d(s) ds d\theta \\ &+ \frac{1}{1-T^+}\int_{t-T(t)}^{t}\int_{\theta}^{t} r_2 \tilde{z}_d^T(s) E^T E \tilde{z}_d(s) ds d\theta \\ &+ \int_{t-T(t)}^{t}\int_{\theta-T(\theta)}^{t} r_2 \tilde{z}_d^T(s) E^T E \tilde{z}_d(s) ds d\theta. \end{aligned} \quad (39)$$

If there exists P_1 satisfying the LMI (26) in *Lemma 2*, the derivative of V_p is given as $\dot{V}_p \le -\parallel \tilde{z}_d \parallel^2$. Thus, The derivative of V_2 is given as

$$\begin{aligned} \dot{V}_2 \le & X_d^T(P_2 A_e + A_e^T P_2 + \gamma_2^{-2} P_2 D_e D_e^T P_2 + I)X_d \\ & - \parallel X_d \parallel^2 + \gamma_2^2 \parallel \tilde{z}_d \parallel^2 - (\gamma_2^2+1) \parallel \tilde{z}_d \parallel^2 . \end{aligned}$$

Since the LMI (33) also imply $P_2 A_e + A_e^T P_2 + \gamma_2^{-2} P_2 D_e D_e^T P_2 + I < 0$, we have $\dot{V}_2 \le -\parallel X_d \parallel^2 - \parallel \tilde{z}_d \parallel^2$. From the Lyapunov-Krasovskii theorem, $\lim_{t\to\infty} X_d, \tilde{z}_d = 0$ is achieved. From the equations (34)(35) and $\lim_{t\to\infty} X_d = 0$, it is achieved that $\lim_{t\to\infty} X = 0$. Namely, the position coordination is achieved. □

This theorem shows that the control objective 1) and 2) are achieved. To achieve the control objective 3) i.e. force reflection, it is required that the certain condition is satisfied as shown in following proposition.

Proposition 1. The force reflection $\tau_{op} = \tau_{env}$ is achieved if $\tilde{z}_d = 0$, $\dot{q}_{sd} = \dot{q}_{md} = \ddot{q}_{sd} = \ddot{q}_{md} = 0$ are satisfied.

This proposition imply that the accurate prediction is required to achieve static force reflection.

5. EXPERIMENTAL EVALUATION

In this section, several experiments are performed to evaluate the effectiveness of proposed predictive PD control. We validate the tracking performance, position coordination and force reflection. To analyze the behavior of system when the delay increases, the experiments are carried out with several delay values. The experiments were carried out on a pair of identical direct-drive planar 2 link revolute-joint robots as shown in Fig. 2. We measure the operational torque τ_{op} and τ_{env} using the force sensors. We use dSPACE as a real-time calculating machine and

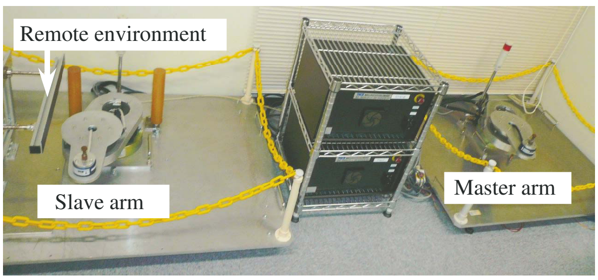

Fig. 2. Experimental setup

1[ms] sampling rate is obtained. We use the environment of an aluminum wall covered by rubber as shown in Fig. 2. All experiments have been done with an artificial time varying delay. The controller parameters are selected as follows.

$$\begin{aligned} &\overline{M}_m = \overline{M}_s = \begin{bmatrix} 1.5 & 0 \\ 0 & 0.5 \end{bmatrix}, \overline{B}_m = \overline{B}_s = \begin{bmatrix} 1.5 & 0 \\ 0 & 0.5 \end{bmatrix} \\ &K_p = \begin{bmatrix} 6 & 0 \\ 0 & 2 \end{bmatrix}, K_d = \begin{bmatrix} 6 & 0 \\ 0 & 2 \end{bmatrix}, K_m = K_s = \begin{bmatrix} 10 & 0 \\ 0 & 5 \end{bmatrix} \\ &\Gamma_m = \Gamma_s = \begin{bmatrix} 1 & 0 & 0 \\ 0 & 1 & 0 \\ 0 & 0 & 1 \end{bmatrix}, \Lambda_m = \Lambda_s = \begin{bmatrix} 5 & 0 \\ 0 & 3 \end{bmatrix} \end{aligned} \quad (40)$$

The gains E_m, E_s are designed according to same procedure as (Pan et al. [2006]) and following parameter is obtained.

$$E_m = E_s = \begin{bmatrix} -0.3196 & 0 & 0.2615 & 0 \\ 0 & -0.3196 & 0 & 0.2615 \\ 0.2635 & 0 & -0.3031 & 0 \\ 0 & 0.2635 & 0 & -0.3031 \end{bmatrix}$$

We have been verified that the matrices A_m, A_s, A_e are stable under above setting. Four kinds of experimental conditions are given.

Case 1: The experiments with small delay
$(T(t) = \overline{T}(t) = 0.25 + 0.1\sin(t))$

Case 1.1: The slave moves without any contact
Case 1.2: The slave contacts with the environment

Case 2: The experiments with large delay
$(T(t) = \overline{T}(t) = 0.5 + 0.3\sin(t))$

Case 2.1: The slave moves without any contact
Case 2.2: The slave contacts with the environment

In Case 1.1, we show the experimental comparison between the proposed method and the PD control method without prediction (Kawada et al. [2008]).

Figs. 3, 4 show the results in case 1.1. Figs. 3(a), 4(a) show the 2nd joint angles and Figs. 3(b), 4(b) show the 2nd joint torques. As shown in these figures, the position coordination is achieved when $\tau_{op} = 0, \tau_{env} = 0$ in both results. However, the position errors caused by the delay can be reduced by using proposed method. Fig. 5 shows results in case 1.2. Figs. 5(a), 5(b), 5(c) show the 2nd joint angles, the 2nd joint torques, the 2nd joint predicted value respectively. As shown in these results, when the slave robot is pushing the environment (5-32[s]) and the conditions in *Proposition 1* ($\parallel \tilde{z}_d \parallel = 0$, $\dot{q}_{sd} = \dot{q}_{md} = \ddot{q}_{sd} = \ddot{q}_{md} = 0$) are satisfied, the environmental force on contact is accurately transmitted to the operator, i.e., force reflection is achieved. Figs. 6,7 show the results in case 2.1, 2.2. These results show that the proposed method achieves position coordination in free-motion even if the delay is large . However, as shown in Fig. 7, the force reflection can not be achieved accurately because the large delay increases the prediction error. It is observed experimentally that the prediction error is decreased and the force reflection can be achieved if $\overline{M}_m, \overline{M}_s, \overline{B}_m, \overline{B}_s$ are increased. However, the increase of $\overline{M}_m, \overline{M}_s, \overline{B}_m, \overline{B}_s$ cause degradation of performance in free motion. Thus, if the delay is large, the design parameter should be tuned carefully.

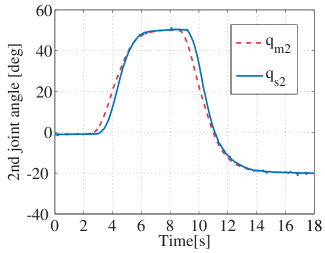

(a) 2nd joint angle

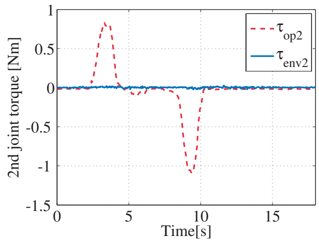

(b) 2nd joint torque

Fig. 3. Experimental results in Case 1.1(proposed method)

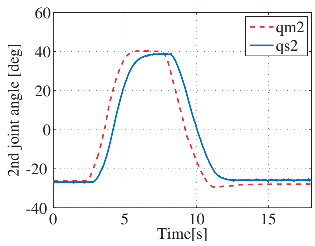

(a) 2nd joint angle

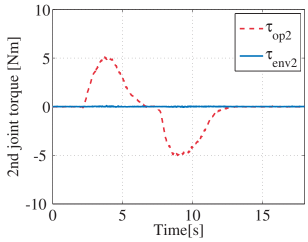

(b) 2nd joint torque

Fig. 4. Experimental results in Case 1.1(without prediction)

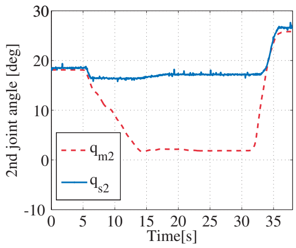

(a) 2nd joint angle

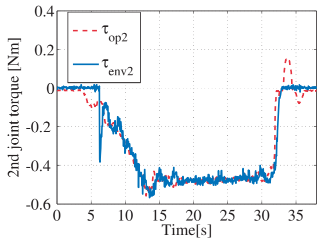

(b) 2nd joint torque

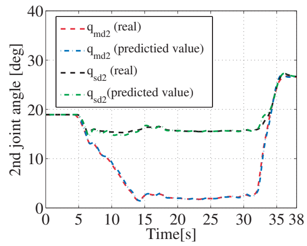

(c) 2nd joint predicted value

Fig. 5. Experimental results in Case 1.2(proposed method)

6. CONCLUSION

In this paper, we addressed a problem of predictive control for nonlinear multi-DOF teleoperation with time varying delay, parametric uncertainties of the robot model, uncertainties of remote environment. The proposed method was combination of the PD control based on predictors and the adaptive impedance control. The stability and the position coordination were guaranteed by using the Lyapunov theorem. Several experimental results showed the effectiveness of our proposed method.

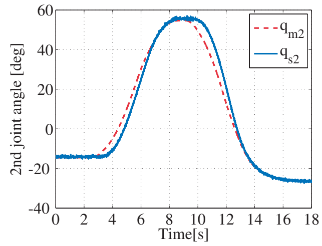

(a) 2nd joint angle

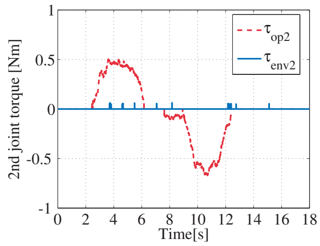

(b) 2nd joint torque

Fig. 6. Experimental results in Case 2.1(proposed method)

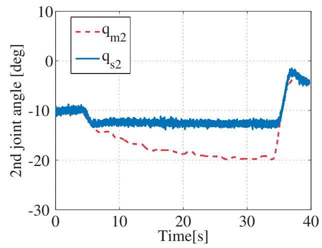

(a) 2nd joint angle

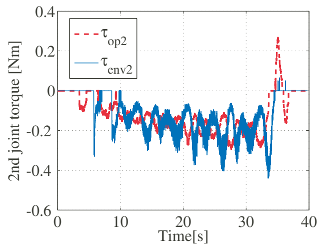

(b) 2nd joint torque

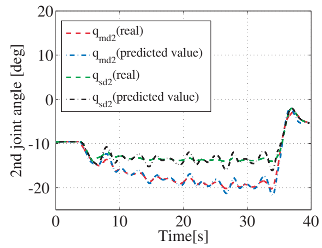

(c) 2nd joint predicted value

Fig. 7. Experimental results in Case 2.2(proposed method)

REFERENCES

P. F. Hokayem and M. W. Spong, "Bilateral teleoperation: an historical survey," *Automatica* Vol. 42, No. 12, pp. 2035-2057, 2006.

N. Chopra, M. W. Spong, S. Hirche and M. Buss, "Bilateral teleoperation over the internet," *Proc. of the 2003 American Control Conference*, pp. 155-160, 2003.

T. Namerikawa and H. Kawada, "Symmetric Impedance Matched Teleoperation with Position Tracking," *Proc. of the 2006 Conference on Decision & Control*, 2006.

H. Kawada and T. Namerikawa, "Bilateral Control of Nonlinear Teleoperation with Time Varying Communication Delays," *Proc. of the 2008 American Control Conference*, 2008(to be published).

Y. J. Pan, C. Canudas-de-Wit, and O. Sename, "A new predictive approach for bilateral teleoperation with applications to drive-by-wire systems," *IEEE Trans. Robot. Autom.*, Vol.10, No.6, pp. 1146-1162, 2006.

S. Sirouspur, A. Shahdi, "Model Predictive Control for Transparent Teleoperation under Communication Time Delay," *IEEE Trans. Robot. Autom.*, Vol.22, No.6, pp. 1131-1145, 2006.

W. S. Lu and Q. H. Meng, "Impedance Control with Adaptation," *IEEE Trans. Robot. Autom.*, Vol.7, No.3, pp. 408-415, 1991.

K. Kosuge, H. Murayama, and K. Takeo, "Bilateral Feedback Control of Telemanipulators via Computer Network," *IEEE International Conference on Intelligent Robots and Systems* Vol. 3, pp. 1380-1385, 1996.